



HAL
open science

Poly(N-cyanoethylacrylamide), a new thermoresponsive homopolymer presenting both LCST and UCST behavior in water

Nicolas Audureau, Fanny Coumes, Jutta Rieger, François Stoffelbach

► **To cite this version:**

Nicolas Audureau, Fanny Coumes, Jutta Rieger, François Stoffelbach. Poly(N-cyanoethylacrylamide), a new thermoresponsive homopolymer presenting both LCST and UCST behavior in water. *Polymer Chemistry*, 2022, 10.1039/D2PY00032F . hal-03561216

HAL Id: hal-03561216

<https://hal.sorbonne-universite.fr/hal-03561216v1>

Submitted on 8 Feb 2022

HAL is a multi-disciplinary open access archive for the deposit and dissemination of scientific research documents, whether they are published or not. The documents may come from teaching and research institutions in France or abroad, or from public or private research centers.

L'archive ouverte pluridisciplinaire **HAL**, est destinée au dépôt et à la diffusion de documents scientifiques de niveau recherche, publiés ou non, émanant des établissements d'enseignement et de recherche français ou étrangers, des laboratoires publics ou privés.

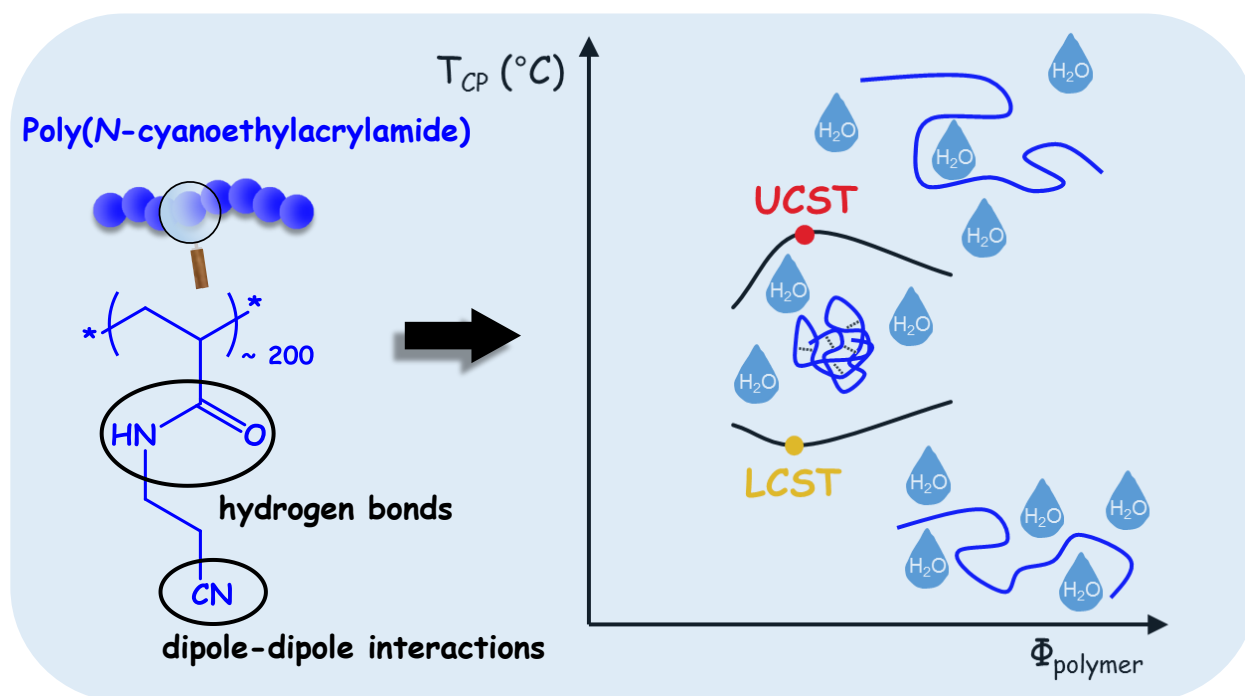
Poly(*N*-cyanoethylacrylamide), a new thermoresponsive homopolymer presenting both LCST and UCST behavior in water

Nicolas Audureau, Fanny Coumes, Jutta Rieger*, François Stoffelbach*

Sorbonne Université, CNRS, UMR 8232, Institut Parisien de Chimie Moléculaire (IPCM), Polymer Chemistry Team, 4 Place Jussieu, 75252 Paris Cedex 05, France

E-mail: jutta.rieger@sorbonne-universite.fr; francois.stoffelbach@sorbonne-universite.fr

FIGURE FOR TOC



Text for TOC

Novel dual thermoresponsive *N*-cyanoethylacrylamide (CEAm)-based (co)polymers synthesized by RAFT polymerization display a lower critical solution temperature (LCST) and an upper critical solution temperature (UCST) in water

Abstract

We have recently demonstrated that poly(*N*-cyanomethylacrylamide) (PCMAm) synthesized by reversible addition-fragmentation chain transfer (RAFT) radical polymerization exhibits a typical upper critical solution temperature (UCST)-type transition in water with a very small hysteresis between cooling and heating steps, and that the cloud point (T_{CP}) of PCMAm is strongly molar mass dependent. In this research article, we have extended the study of the *N*-cyanoalkylacrylamide family by studying for the first time the RAFT polymerization of *N*-cyanoethylacrylamide (CEAm), which differs from CMAm by the presence of a second methylene group between the amide and cyano functional groups. Thereby, novel thermoresponsive homopolymers of CEAm displaying either a lower critical solution temperature (LCST) or both a LCST and an UCST (with $LCST < UCST$) in pure water were obtained. Interestingly, the transitions were sharp and reversible with low hysteresis. The investigation of PCEAm with a $DP_n \sim 200$ at different concentrations proposed a closed-loop phase diagram. Finally, the effect of the addition of comonomer units (CMAm or acrylamide) in the polymer chains on the window of solubility and their interplay in achieving tunable double thermoresponsiveness are also presented.

1. Introduction

Thermoresponsive polymers presenting an upper and/or a lower critical solution temperature, namely UCST and LCST respectively, in water are very interesting to design smart materials¹ in various fields, in particular as drug delivery systems². Indeed, it has been demonstrated that UCST-carriers can efficiently encapsulate drugs, which can be released in a controlled way by the temperature.³ UCST-type polymers are divided in two classes: ionic polymers and non-ionic polymers.^{4,5,6,7,8,9,10,11,12,13} Non-ionic polymers have the advantage to be less sensitive to pH and

ionic strength. Among them, poly(acrylamide-*co*-acrylonitrile) (P(Am-*co*-AN)) has been widely studied.^{14,15,16,17, 18,19} The UCST-type transition of this copolymer is mainly caused by dipole-dipole interactions between the cyano groups of the AN units in addition to hydrogen bonds between the Am units.²⁰ Increasing the content of AN in the composition of the copolymer (F_{AN}) leads therefore to an increase of the cloud point (T_{CP}), which can be finely tuned as long as a good control of F_{AN} is achieved.^{9,21} Yet, the use of AN poses some technical issues especially because it is highly volatile,²⁰ and its reactivity during copolymerization is different from that of Am²² resulting in an inhomogeneous monomer distribution within P(Am-*co*-AN) copolymer chains (in the case of reversible deactivation radical polymerization, RDRP) or in a compositional heterogeneity in polymer chains (in the case of conventional radical polymerization). We recently designed a new UCST-type polymer, inspired by the aforementioned copolymer combining the amide and cyano functional groups in a single monomer unit, namely *N*-cyanomethylacrylamide (CMAM).^{23,24} Copolymerization of CMAM with hydrophilic comonomers such as Am and acrylic acid, allowed to expand the T_{CP} range of the copolymers from ~20 to 85 °C. Motivated by the surprisingly versatile thermoresponsiveness of PCMAM and its copolymers, in this present work we investigated for the first time the thermoresponsiveness of a related polymer, namely poly(*N*-cyanoethylacrylamide) (PCEAm). Thanks to its structural similarity to PCMAM, we postulated that this polymer might also exhibit interesting thermoresponsive properties. Indeed, CEAm differs from CMAM by an additional methylene group between the amide and cyano functional groups, and like CMAM it can be straightforwardly synthesized. While only few patents can be found in literature regarding its free radical (co)polymerization with other (meth)acrylamides or acrylonitrile^{25,26,27}, there is no report so far on its controlled radical polymerization nor any study on its possible thermosensitive properties. We report here for the first time the polymerization of CEAm by RAFT-RDRP and systematically studied the thermoresponsive behavior of the resulting

polymers in water. Notably, the impact of the number-average degree of polymerization (DP_n), the polymer concentration, the presence of salt and the addition of comonomers (CMAm or Am) in the polymer chain is investigated.

2. Experimental part

2.1. Materials

3-Aminopropionitrile (ABCR, 98%), acryloyl chloride (Aldrich, 97%), acrylamide (Am, Aldrich, $\geq 99\%$), 2,2'-azobis(isobutyronitrile) (AIBN, Aldrich, $\geq 98\%$), 2,2'-azobis[2-(2-imidazolin-2-yl)propane]dihydrochloride (VA-044) (Aldrich, 98 %), triethylamine (Alfa Aesar, $\geq 99\%$) and *N,N*-dimethylformamide (DMF, VWR, Normapur) were used as received. *N*-cyanomethylacrylamide (CMAm) and ethyl 2-(butylthiocarbonothioylthio) propanoate (CTA-1) were synthesized according to protocols previously described.^{28,29}

2.2. Synthesis

Synthesis of *N*-cyanoethylacrylamide

3-Aminopropionitrile (14.4 mL; 197 mmol) and triethylamine (30.5 mL; 219 mmol) were mixed in 125 mL of ethyl acetate in an ice bath under inert atmosphere. Acryloyl chloride (16 mL; 197 mmol) was added in three steps at 0 °C. The reaction medium was stirred during 1h at room temperature, filtered and evaporated under reduced pressure at 40 °C. The crude product was purified through silica gel column chromatography in ethyl acetate ($R_f = 0.35$). (Yield = 78%). ¹H NMR (**Figure S2**) (300 MHz, CDCl₃, δ (ppm)): 6.48 (broad, 1H, NH), 6.28 (d, 1H, C=CH₂), 6.14 (q, 1H, C=CH), 5.71 (d, 1H, C=CH₂), 3.56 (q, 2H, NHCH₂), 2.66 (t, 2H, CH₂CN). ¹³C NMR

(**Figure S2**) (100 MHz, CDCl₃, δ (ppm)): 166.3 (C=O), 130.2 (CH₂=CH), 127.4 (CH₂=CH), 118.4 (CN), 35.8 (NHCH₂), 18.4 (CH₂CN).

RAFT homopolymerizations of *N*-cyanoethylacrylamide in DMF

In a typical experiment (**P3**, **Table 1**), 0.709 g (5.72 mmol) of *N*-cyanoethylacrylamide, 0.25 mg (1.50 μ mol) of 2,2'-azobis(isobutyronitrile) (AIBN), 3.9 mg (15 μ mol) of ethyl 2-(butylthiocarbonothioylthio)propanoate (CTA-1) and 2.8 g of DMF were introduced in a septum-sealed 5 mL round-bottom flask, immersed in an ice bath and purged for 30 min under argon. The flask was then placed in a thermostated oil bath at 70 °C for 3.6 h. Aliquots were taken and analyzed by ¹H NMR to determine the monomer conversion. The polymerization was quenched by exposure to air and placing into an ice bath. The polymer was precipitated in chloroform, filtered over a Büchner funnel and dried under vacuum at 40 °C.

RAFT copolymerizations of *N*-cyanoethylacrylamide with CMAM or Am in DMF

In a typical experiment (**P8**, **Table 2**), 4.1 mg (15 μ mol) of ethyl 2-(butylthiocarbonothioylthio)propanoate (CTA-1), 0.43 mg (2.56 μ mol) of AIBN, 0.479 g (3.86 mmol) of CEAm and 47.8 mg (0.43 mmol) CMAM were dissolved in 2.1 g of DMF in a septum-sealed 5 mL round bottom flask. The mixture was purged with argon for 30 min in a chilled water bath. The flask was immersed in a thermostated oil bath at 70 °C for 155 min. The individual monomer conversions were kinetically followed by taking aliquots from the reaction media and analyzing them by ¹H NMR. The polymerization was quenched by exposure to air and placing the flask into an ice bath. The polymer was precipitated in chloroform, filtered over a Büchner funnel and dried under reduced vacuum at 40 °C.

2.3. Characterization techniques

^1H NMR spectra were recorded in D_2O , DMSO-d_6 or in CDCl_3 at 300 K on a Bruker 300 MHz or 400 MHz spectrometer in 5 mm diameter tubes.

SEC measurements were carried out at 60 °C in DMF (+LiBr, 1 g L^{-1}) as mobile phase at a flow rate of 0.8 mL min^{-1} using toluene as a flow rate marker. Polymer solutions were prepared at a concentration of 5 mg mL^{-1} and filtered through a 0.2 μm PTFE membrane. 100 μL of solution was injected for each measurement for analysis. The separation system was composed of two PSS GRAM 1000 Å columns (8×300 mm; separation limits: 1 to 1000 kg mol^{-1}) and one PSS GRAM 30 Å (8×300 mm; separation limits: 0.1 to 10 kg mol^{-1}) coupled with a Tetra Detector Array including a light scattering detector with a Right (90°) and a Low (7°) angle (RALS/LALS) and a laser at 670 nm, a 4-capillary differential viscometer, a differential refractive index detector (RI) and an UV detector. Molar masses (M_n , M_w , respectively the number-average molar mass and the weight-average molar mass) and dispersities ($D = M_w/M_n$) were calculated using OmniSEC 5.12 software with a calibration curve based on narrow PMMA standards (from Polymer Standard Services).

Turbidimetry measurements of PCEAm homopolymers and CEAm-based copolymers in water were performed on a Cary 100 UV-Vis spectrophotometer (Agilent) equipped with a Peltier-type temperature control system (≤ 0.2 °C temperature measurement accuracy) by measuring the transmittance at a wavelength of 670 nm. The heating/cooling rate was maintained constant at 1 °C min^{-1} and all measurements were performed under magnetic stirring. Samples were prepared at a concentration of 1 wt% (unless stated otherwise) by dissolving the purified polymers in ultra-pure water. The cloud points (T_{CP}) were determined at the inflection point.

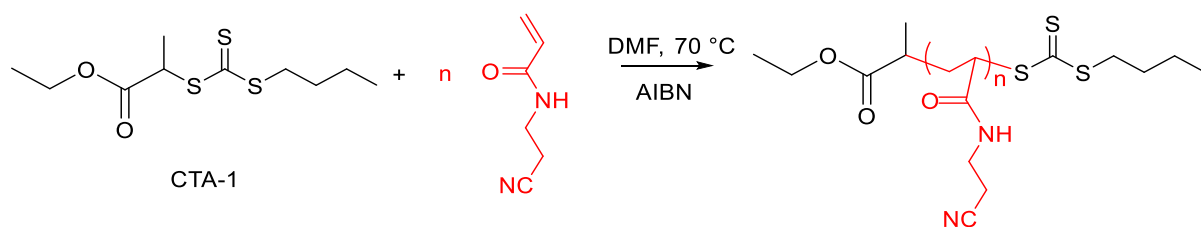
Differential scanning calorimetry (DSC) measurements were performed on a TA instruments Q2000 device. Heating-cooling cycles were successively performed between -50 °C and 250 °C at a rate of 20 °C min⁻¹. Thermogravimetry analysis (TGA) measurements were performed under air at a heating rate of 20 °C min⁻¹ using a TA instruments Q50 to assess its resistance towards degradation.

Dynamic Light Scattering (DLS). The DLS measurements were carried out on a Zetasizer Nano S90 from Malvern (90° angle, 5 mW He–Ne laser at 633 nm).

3. Results and discussion

3.1. Synthesis of PCEAm homopolymers by RAFT polymerization in DMF solution

The CEAm monomer was readily obtained in a one-step procedure by adapting the synthesis procedure developed for CMAM.²³ It consists in an amidation reaction between acryloyl chloride and 3-aminopropionitrile performed in the presence of trimethylamine as a proton trap (**Scheme S1**). After confirming its purity by ¹H and ¹³C NMR (**Figure S2**), we investigated for the first time its ability to be radically homopolymerized in a controlled fashion by RAFT in DMF (**P1-P6, Table 1 and Scheme 1**). 2,2'-Azobis(isobutyronitrile) (AIBN) was chosen as an initiator, and ethyl 2-(butylthiocarboethioylthio)propanoate (CTA-1) was chosen as a trithiocarbonate-type chain transfer agent (CTA) - known to control the polymerization of acrylamide monomers - because they are non-ionic and should therefore minimize the effect of the chain end^{30,31} on the thermoresponsive behavior.



Scheme 1. Synthesis route for PCEAm polymers *via* RAFT polymerization.

CEAm was also polymerized in DMF by free radical polymerization (FRP) - without CTA - using again AIBN as the initiator (**P7**, **Table 1**). The SEC analysis showed that the chain distribution was broad and monomodal, as expected, and the ^1H NMR spectrum of the purified polymer confirmed its supposed structure (**Figure S3**). Concerning the polymerizations performed in the presence of CTA-1, conversions above 50% were generally reached in less than 4 h (**Table 1** and **Figure 1A**). **Figure 1B** shows that the SEC traces evolved toward higher molar masses when increasing the targeted DP_n . The polymerizations were generally well controlled, as evidenced by the symmetric and narrow molecular weight distribution with dispersities ($D = M_w/M_n$) below 1.2 for polymers **P1** to **P4** (**Table 1**) and the experimental molar masses ($M_{n,LS}$) that matched well the theoretical values. However, for the highest molar mass polymers **P5** and **P6** with $DP_n > 300$, the SEC traces were less symmetric, with dispersities around 1.4 and experimental molar masses ($M_{n,LS}$) differing from the expected ones, indicating a progressive decrease in control. The absolute number-average molar mass values ($M_{n,LS}$) were determined by SEC equipped with an in-line static light scattering (SLS) detector (**Table 1**). A dn/dC value of 0.088 mL g^{-1} was determined (for details see **SI** and **Figure S1**). For polymers **P5** and **P6**, the $M_{n,LS}$ were significantly lower than the expected values. This might be explained by irreversible transfer reactions occurring during the polymerization, which have a greater impact on the DP_n when high DP_n values are targeted reducing the $M_{n,LS}$ compared to the expected $M_{n,th}$. Indeed, for **P5** and **P6**, the chromatograms were asymmetric showing a tailing towards lower molar masses (see **Figure 1B**).

Furthermore, additional SEC analyses using combined RI and UV in-line detectors further confirmed the efficiency of the desired chain transfer reaction: the RI and UV response (at 309 nm) in the SEC chromatogram of sample P1 (**Figure 1C**) perfectly overlay suggesting that the trithiocarbonate functionality, which strongly absorbs at this wavelength,³² is present over the whole chain distribution. In addition, ¹H NMR in D₂O (**Figure S4**) and DMSO-d₆ (**Figure S5**) confirmed the presence of the CTA-1 in the polymer chains with the CH₃ end-chain of CTA-1 visible at $\delta = 0.9$ -1.0 ppm (see the note after the Figure S5 in the supporting information). The combined SEC and ¹H NMR results confirm thus a chain end-functionalization by the CTA-1 close to 100%.

Furthermore, we showed that the RAFT-mediated polymerization of CEAm could successfully be reproduced (*e.g.*: the replica of **P4** (Table 1) named **P4bis**, see data in the SI, **Table S1** and **Figure S6**) demonstrating the robustness of the polymerization conditions.

Table 1. Experimental conditions and results for the RAFT-mediated polymerizations of CEAm performed at 20 wt% in DMF[#]

Expt.	[CEAm] ₀ / [CTA-1] ₀	Time (h)	Conv. ^a (%)	DP _{n,th} ^b	M _{n,th} ^b (kg mol ⁻¹)	DP _{n,NMR} ^c	M _{n,NMR} ^c (kg mol ⁻¹)	M _{n,SEC} ^d (kg mol ⁻¹)	D ^d	M _{n,LS} ^e (kg mol ⁻¹)	T _{CP} ^f (°C)	
											LCST	UCST
P1	117/1	3.0	76	89	11.3	90	11.4	21.3	1.09	13.7	Soluble	Soluble
P2	220/1	1.6	72	158	19.9	159	20.0	31.5	1.15	20.6	(48/55) [†]	(58/65) [†]
P3	390/1	3.6	50	195	24.4	205	25.7	35.8	1.20	21.1	39/43	75/79
P4	350/1	1.6	59	207	25.9	212	26.6	36.8	1.18	23.3	41/44	77/79
P5	380/1	8.6	87	331	41.3	-	-	44.1	1.34	31.3	31/33	N.O.
P6	815/1	8.9	62	505	62.9	-	-	54.8	1.44	38.6	20/25	N.O.
P7 [*]	-	1.2	93	-	-	-	-	58.1	2.38	42.4	10/14	N.O.

[#] Polymerizations were performed at 70 °C in presence of the RAFT agent CTA-1 using AIBN as a radical initiator at an initial molar ratio of CTA-1/AIBN: 1/0.1. ^{*} Free radical polymerization (without RAFT agent) at an initial molar ratio of CEAm/AIBN: 180/1. ^a Determined by ¹H NMR analysis. ^b Theoretical number-average degree of polymerization, DP_{n,th}, and theoretical number-

average molar mass, $M_{n,th}$, calculated using the experimental conversions. ^c Number-average degree of polymerization, $DP_{n,NMR}$, and number-average molar mass, $M_{n,NMR}$, determined by ¹H NMR analysis of the purified polymer using the signal of the CH₃ end-chain of CTA-1 (for P5 and P6, the determination of $DP_{n,NMR}$ is not accurate due to the low signal of the CH₃ end-chain of CTA-1). ^d Number-average molar mass, M_n , and dispersity, \mathcal{D} , determined by SEC in DMF (+ LiBr 1 g L⁻¹) with a PMMA calibration. ^e Determined by SEC using a LS detector and the experimental dn/dC value: 0.088 mL g⁻¹ (for details see SI and Figure S1). ^f Determined in water by turbidimetry at 1 wt%, on 1st cooling/2nd heating. N.O.: not observed in the studied temperature range (10-80 °C). [†] Partial thermal transition (see Figure 2).

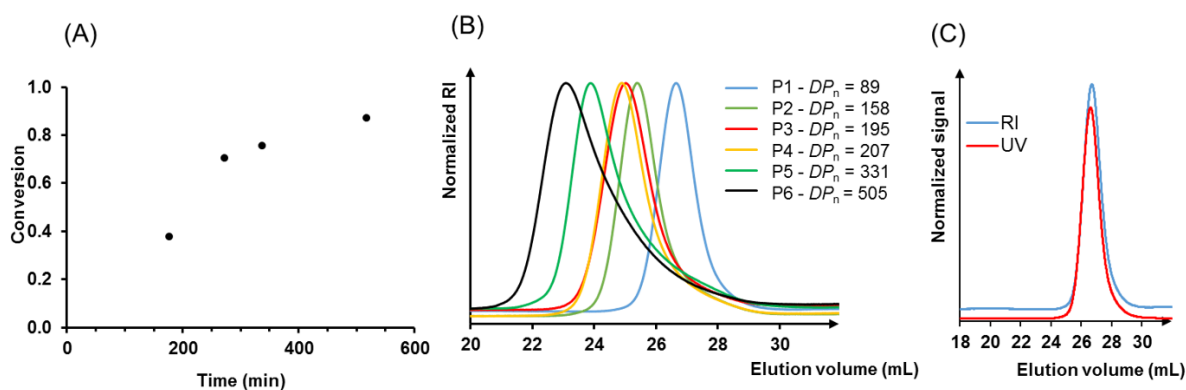


Figure 1. (A) Monomer conversion during the RAFT polymerization of CEAm monitored by ¹H NMR in CDCl₃ (P5, Table 1). (B) Evolution of the SEC chromatograms in DMF (+ LiBr) for the RAFT polymerizations of CEAm targeting different DP_n (P1 to P6, Table 1). (C) SEC traces obtained in DMF (blue: refractive index (RI) detector and red: UV detector at $\lambda = 309$ nm) for PCEAm₈₉ (P1, Table 1).

As our study is the first report on PCEAm, we wanted to determine its thermal properties, using dry powder of polymer **P7**. Thermogravimetry analysis (TGA) (**Figure S7A**) evidenced a thermal degradation at about 350 °C, which is higher than the one of PCMAm (250 °C)²³. By differential scanning calorimetry (DSC), a glass transition temperature (T_g) (**Figure S7B**) of 64 °C was determined, which is considerably lower than the T_g of PCMAm (200 °C). This difference can be explained by the presence of an extra methylene group in the CEAm monomer units, which

increases the free volume around the backbone and the mobility of the polymer side-chain, reducing thus the packing of the polymer chain.³³

3.2. Study of the thermal properties of PCEAm in aqueous solution

The different PCEAm samples were dissolved at a concentration of 1 wt% in pure water in order to examine their thermoresponsiveness by turbidimetry (**Figure 2**). For all polymers with $DP_n \geq 195$, turbidimetry measurements displayed a clear typical LCST-type transition: the transparent polymer solution became turbid upon heating, evidencing chains aggregation. We observed that the cloud point ($T_{CP,LCST}$) decreased almost linearly from 48 to 20 °C as the DP_n increased from 158 to 505 (**Figure S8**). This decrease in solubility with DP_n corresponds to the expected increase in the free energy of mixing ΔG_m for longer polymer chains. Similar observations were made for other LCST-type homopolymers such as poly(*N*-isopropylacrylamide) (PNIPAm)³⁴, poly(*N,N*-diethylacrylamide)³⁵, poly(2-(*N,N*-dimethylamino)ethyl methacrylate)³⁶, poly(2-(*N*-morpholino)ethyl methacrylate)³⁶, poly(oligo(ethylene glycol) methacrylate)³⁷, poly(*N*-vinylpiperidone)³⁸ and poly(*N*-vinylcaprolactam)³⁹. In addition, an UCST-type transition was also observed for samples with $158 \leq DP_n \leq 207$: the turbid solution evolved to a transparent solution upon heating. DLS measurements confirmed that the polymer chains were mainly molecularly dissolved below the $T_{CP,LCST}$ and above the $T_{CP,UCST}$ (**Figure S6B**), while aggregates were formed in between. Similar to the LCST-type cloud point ($T_{CP,LCST}$), the clearing point ($T_{CP,UCST}$) was also influenced by the DP_n . It increased from 58 to 77 °C with the DP_n increasing from 158 to 207. Previously, we had observed the same trend for PCMAm²³ and others described the same dependency for other UCST-type polymers, for instance poly(*N*-acryloylasparaginamide).⁴⁰ Finally, the shortest polymer, with DP_n (89), was soluble over the whole temperature range, no transition was observed, at least not at 1 wt%. Interestingly, PCEAm displayed LCST (and UCST)

thermal transitions in water only for sufficiently long polymer chains, with DP_n beyond 90, whereas PCMAm displayed UCST-type thermal transition only for sufficiently short polymer chains with a critical lower DP_n far below 180.

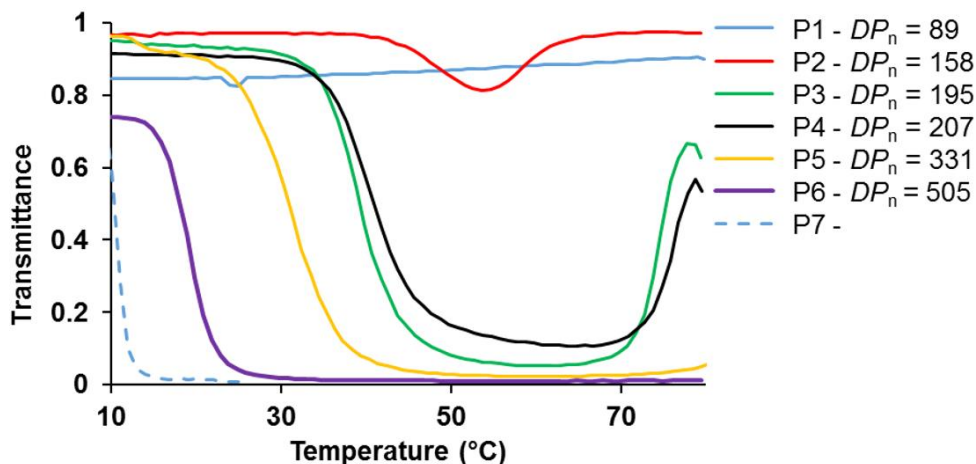


Figure 2. Turbidity curves (first cooling) of PCEAm polymers with various DP_n at 1 wt% in water (Table 1).

Two cycles of turbidimetry measurements were performed to assess the reproducibility and reversibility of these peculiar thermosensitive properties. **Figure S9** shows that the dual temperature-response of sample **P3** is reversible and no significant modification of the T_{CP} over the cycles was observed. In addition, the hysteresis observed for each T_{CP} (LCST and UCST-like) between heating and cooling steps was very small and did not exceed 4 °C.

The influence of the concentration over the T_{CP} was also investigated. **Figure 3A** shows the turbidimetry profiles obtained for sample **P4** analyzed at various concentrations (1 to 6 wt%). At lower concentration (0.5 wt%), visually no thermal transition was observed. These analyses permitted the tentative construction of a phase diagram displayed in **Figure 3B**. The data suggest a closed-loop-type phase diagram with $LCST < UCST$, where the polymer is insoluble within the

loop and soluble outside. It should be noted that for the sample at 2 wt% a start of a thermal transition was observed above 90 °C, but it was not possible to properly determine the $T_{CP,UCST}$. We therefore decided to indicate an estimated T_{CP} around 100 °C in the phase diagram of **Figure 3B**.

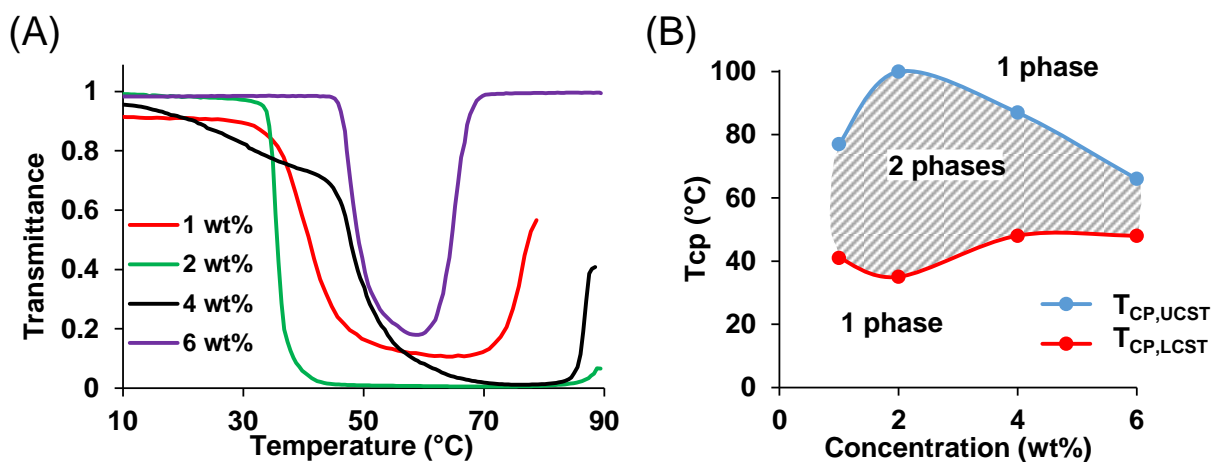


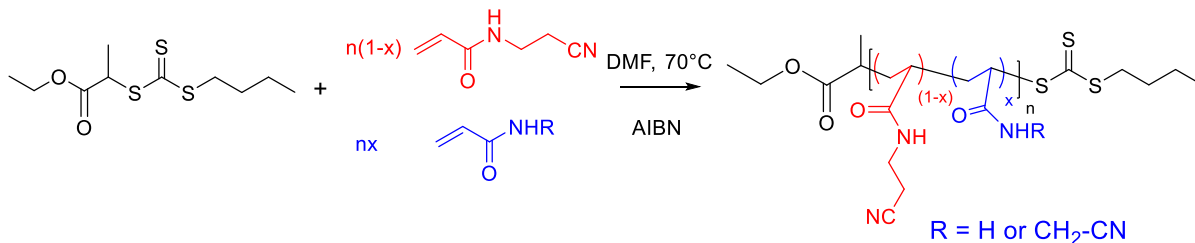
Figure 3. (A) Turbidity curves of PCEAm₂₀₇ (P4, Table 1) in water at various concentrations (cooling step) and (B) phase diagram constructed over the concentration range studied, blue symbols for the UCST type T_{CP} and red symbols for the LCST type T_{CP} .

Finally, to investigate the influence of the NaCl concentration on the thermoresponsiveness of PCEAm, turbidimetry measurements of PCEAm₂₁₁ (**P4bis**, **Table S1**) aqueous solutions at 1 wt% were done at increasing NaCl concentrations. As shown in **Figure S10**, using a 10 mM saline solution, the $T_{CP,LCST}$ increased from ~40 to ~55 °C and the $T_{CP,UCST}$ slightly decreased from ~77 to ~70 °C. In presence of a higher concentration of NaCl (150 mM), the dual LCST-UCST thermoresponsiveness completely disappeared. The homopolymer was no longer sensitive to modification in temperature, presumably because polymer-polymer interactions were attenuated, therefore the supposed $T_{CP,LCST}$ becoming higher than the $T_{CP,UCST}$. For other non-ionic UCST-type polymers, namely PCMAm²³, poly(*N*-acryloyl glycineamide)³¹ and P(Am-*co*-AN)²⁰, such a

decrease in the $T_{CP,UCST}$ with increasing ionic strength has already been observed. For LCST-type polymers such as PNIPAm, it is well-known that the $T_{CP,LCST}$ is lowered by the addition of the NaCl due to the “salting out” effect.⁴¹ In our case, the addition of NaCl induces the opposite effect (salting in) thus explaining the observed behavior.

3.3. Synthesis and characterization of P(CEAm-co-X) statistical copolymers (with X = Am or CMAM)

The observed dual LCST-UCST thermoresponsiveness behavior of PCEAm was unexpected and highly interesting, as it occurred in the customary temperature range. Whereas LCST-related cloud points ($T_{CP,LCST}$) were observed roughly between 10 and 40 °C, the UCST-related clearing points ($T_{CP,UCST}$) were above 70 °C. It is well known that the transition temperatures of thermoresponsive homopolymers can be tuned by copolymerization with adequate comonomers.^{8,9,19,21,23,42} In order to tune the transition temperatures of PCEAm, we therefore copolymerized CEAm with two monomers (**Scheme 2**), namely CMAM and Am that should modify the solubility of the resulting copolymer. While Am is a highly hydrophilic comonomer, known to increase LCST⁴³ and decrease UCST^{9,42}, CMAM was selected for its structural similarity to CEAm, which might promote interactions between both comonomers and possibly lead to complex thermoresponsive properties.



Scheme 2. Synthesis route for P(CEAm-co-X) copolymers (with X = Am or CMAM) *via* RAFT polymerization.

Using the same polymerization conditions as for CEAm, two copolymers with CMAM in feed molar ratios ($f_{\text{CMAM},0}$) of 0.08 and 0.48 were prepared (**Table 2**, copolymers **P8** and **P9**).

Table 2. Experimental conditions for the synthesis of P(CEAm-*co*-CMAM) copolymers in the presence of CTA-1 and their characterisation[#]

Expt.	mol% of CMAM ^a	[M] ₀ /[CTA-1] ₀ /[AIBN] ₀	Time (min)	Conv. ^b (mol%)		mol% of CMAM ^c	$F_{\text{CMAM}}^{\text{d}}$	$DP_{\text{n,th}}^{\text{e}}$	$M_{\text{n,th}}^{\text{e}}$ (kg mol ⁻¹)	$M_{\text{n,SEC}}^{\text{f}}$ (kg mol ⁻¹)	\mathcal{D}^{f}
				CEAm	CMAM						
P3	0	390/1/0.1	216	50	-	0	0.00	195	24.4	35.8	1.20
P8	8	280/1/0.1	155	68	74	9	0.10	192	23.8	33.6	1.26
P9	48	265/1/0.1	85	60	64	50	0.50	164	19.5	28.9	1.56
P10	100	230/1/0.2	360	-	82	100	1.00	189	21.1	22.2	1.47

[#]Polymerizations were performed at 20 wt% in DMF at 70 °C in presence of the RAFT agent CTA-1 and AIBN as a radical initiator. ^a Initial mol% of CMAM in the mixture of monomers. ^b Individual monomer conversions determined by ¹H NMR analysis. ^c mol% of CMAM in the copolymer deduced from the experimental conversions. ^d molar fraction of CMAM in the purified copolymer deduced from ¹H NMR analysis (see an example in **Figure S12**). ^e Theoretical number-average degree of polymerization, $DP_{\text{n,th}}$, and theoretical number-average molar mass, $M_{\text{n,th}}$, calculated using the experimental conversions. ^f Number-average molar mass M_{n} and dispersity, \mathcal{D} , determined by SEC in DMF (+ LiBr 1 g L⁻¹) with a PMMA calibration.

Monitoring of the copolymerizations by ¹H NMR revealed that the individual monomer conversions (**Figure S11A**) were close without significant variation of the monomers feed composition, suggesting similar reactivity for CEAm and CMAM. This result could be expected since their chemical structures are very close. The molar composition of CMAM in the copolymers (F_{CMAM}) were determined by ¹H NMR on the purified polymers (see an example for **P8** in **Figure S12**). As expected, they were in good agreement with the molar composition determined from the experimental conversions and close to the feed composition (see **Table 2**). SEC chromatograms (**Figure S11B**) revealed a good polymerization control for the copolymer with the low amount of CMAM ($f_{\text{CMAM},0} = 0.08$) along with symmetrical chromatograms and narrow distribution ($\mathcal{D} = 1.26$), similar to the PCEAm homopolymer. For the copolymerization in the presence of higher

amount of CMAM ($f_{\text{CMAM},0} = 0.48$), the SEC trace was less symmetrical and the dispersity broadened to $D = 1.56$, similar to the homopolymerization of CMAM.²³

The thermoresponsiveness of these copolymers was investigated by turbidimetry measurement at 1 wt%. **Figure 4** reveals that the copolymer with $F_{\text{CMAM}} = 0.1$ (**P8, Table 2**) retains a double LCST-UCST-type behavior like the corresponding PCEAm homopolymer (**P3, Table 2**). However, a lower $T_{\text{CP,LCST}}$ and a higher $T_{\text{CP,UCST}}$ were determined, *i.e.* the window of solubility is reduced. In contrast, the copolymer with $F_{\text{CMAM}} = 0.5$ (**P9, Table 2**) lost completely the typical double thermoresponsive behavior of the corresponding homopolymer PCEAm (**P3**): the solution remained turbid over the whole temperature range studied, revealing the poor solubility of the P(CEAm_{0.5}-*co*-CMAM_{0.5}) copolymer in water, at least at 1 wt%, similar to the PCMAm homopolymer (**P10, Table 2**). In view of these results, we can thus conclude that the insertion of CMAM as a comonomer increases chain interactions, presumably through dipole-dipole interactions of the cyano groups present in both comonomers.

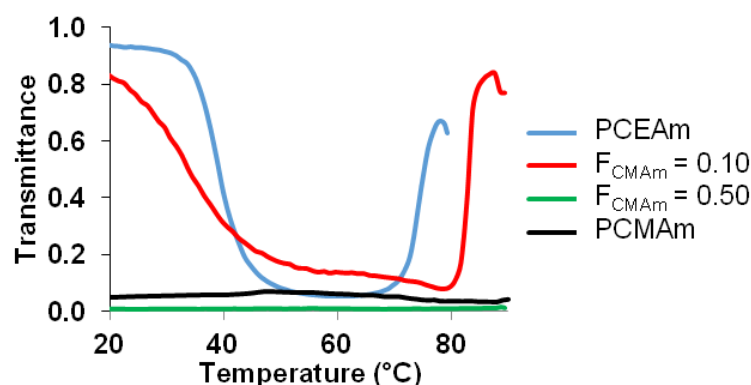


Figure 4. Turbidity curves of P(CEAm-*co*-CMAM) at two different F_{CMAM} , PCMAm and PCEAm (**P3** and **P8-P10, Table 2**) at 1 wt% in water.

To explain the origin of the dual transition observed for PCEAm, which is preserved but modified when a low quantity of CMAM units (9 mol%) was inserted, we suppose that upon heating to intermediate temperatures, a LCST-type coil-globule transition happens driven by dipole-dipole and hydrophobic interactions. Further heating might then (i) destabilize the dipole-dipole interactions between the cyano groups and (ii) break the inter- and intrachain H-bonds between amide groups. Thereby, polymer-polymer interactions are reduced in favour of interactions with water molecules, which leads to redissolution of the polymer chains.

In a second set of experiments, CEAm and Am were also copolymerized using the same polymerization conditions as before (**Scheme 2**). The molar concentration of Am in the feed was 2.0 or 8.4 mol% (**Table S2**), keeping constant the total monomer concentration at 20 wt%, and targeting $DP_n = 200$. Kinetic monitoring of the polymerizations by ^1H NMR showed that the copolymerizations proceeded without significant variation of the copolymer composition (**Figure S13**). Indeed, the calculated molar percentages of Am in the copolymers determined by ^1H NMR at any conversion remained close to the initial ones (final values given in **Table S2**). This suggests a very similar reactivity of both monomers. After purification by precipitation in chloroform, the copolymers were characterized by ^1H NMR and SEC (**Table S2** and **Figures S14 and S15**). Generally, polymerization control was reached for all compositions: the SEC chromatograms were symmetric and low molar mass dispersities ($D < 1.3$) were obtained. In addition, the molar fraction of Am in the copolymers determined by ^1H NMR (F_{Am} , **Table S2**) was very close to the initial molar fraction of Am in the feed, indicating a random copolymerization mechanism.

The thermoresponsiveness of the copolymers was investigated by turbidimetry measurement at 1 wt% (not shown). In contrast to the reference homopolymer PCEAm (**P4bis**, **Table S2**), the copolymers containing 2 or 9 mol% of Am (**P11** and **P12**, **Table S2**) were soluble in water over

the whole temperature range studied, no thermal transition was observed. The insertion of Am as a hydrophilic comonomer – even in very small proportion – is thus sufficient to erase completely the thermosensitivity. The influence of the concentration over the T_{CP} was also investigated at higher concentration (4 wt%). **Figure S16** shows the turbidimetry profiles obtained for samples **P4bis**, **P11** and **P12** (**Table S2**) analyzed at 4 wt% in water. At this higher concentration, the copolymer with $F_{Am} = 0.02$ (**P11**, **Table S2**) exhibits again a double LCST-UCST-type behavior (also visually observed, see **Figure S17**), whereas for the copolymer with $F_{Am} = 0.09$ (**P12**, **Table S2**) the solution remained limpid over the whole temperature range studied. The results evidenced that the CEAm/Am comonomer fraction within the polymer chains and the concentration of the copolymer in water have a great impact on the thermoresponsiveness.

4. Discussion and conclusions

In conclusion, we have shown for the first time that it is possible to polymerize CEAm in a controlled way by RAFT-mediated radical polymerization. Most importantly, we have evidenced that PCEAm homopolymers may exhibit LCST and UCST-type transitions in pure water that are fully reversible. We have shown that the temperature-response was strongly molar mass dependent. For molar masses above 30 kg mol^{-1} only a LCST could be measured, whereas the shortest polymer with a molar mass around 14 kg mol^{-1} was water-soluble at 1 wt%, at least over the studied temperature range (10 to $80 \text{ }^\circ\text{C}$). Polymers of intermediate molar mass exhibited a dual LCST and UCST temperature response, with $\text{LCST} < \text{UCST}$. In more detail, the LCST-type transition at 1 wt% in water increased from 10 to $48 \text{ }^\circ\text{C}$ for molar masses decreasing from 60 to 20 kg mol^{-1} , whereas the UCST-type transition increased from $58 \text{ }^\circ\text{C}$ to above $77 \text{ }^\circ\text{C}$ when the molar mass increased from roughly 20 kg mol^{-1} to 25 kg mol^{-1} . Compared to PCMAm which possesses a clear

UCST-type transition only for molar masses below $\sim 10 \text{ kg mol}^{-1}$, the thermoresponsive behavior of PCEAm is thus more versatile. It should be noted that such a dual LCST-UCST thermoresponsive behavior with $\text{LCST} < \text{UCST}$, in pure water in standard conditions ($0\text{--}100 \text{ }^\circ\text{C}$, $P = 1 \text{ atm}$), has only scarcely been reported for homopolymers.^{44,45,46,47} Indeed, to the best of our knowledge, soluble-insoluble-soluble transitions were seen in pure water for only four *homopolymers*: poly(2-hydroxyethyl methacrylate)⁴⁴ with a DP_n of about 25, poly(dimethyl 3,3'-(((1-(2-hydroxy-3-(methacryloyloxy)propyl)-1H-1,2,3-triazol-4-yl)methyl)azanediyl) dipropanoate) modified after polymerization by esterification of all hydroxyl groups with succinic anhydride⁴⁵, a homopolypeptide with di(ethylene glycol) linkages and tributylphosphonium iodide⁴⁶ with a DP_n of 48 and 80, and poly(methyl 2-acetamidoacrylate)⁴⁷ with a DP_n of about 160. There are more reports on copolymers, either *statistical copolymers* - such as (poly[(*N*-sulfopropylbetaine)propyl 2-acrylamidoisobutyramide]_x-*co*-(*N*-benzyl 2-acrylamidoisobutyramide)_y-*co*-(*N*-tetrahydrofurfuryl 2-acrylamidoisobutyramide)_z] obtained by postpolymerization modification reactions of poly(2-vinyl-4,4-dimethylazlactone)⁴⁸, or vinyl alcohol-based copolymers obtained after partial butyralization ($< 13 \text{ mol}\%$)⁴⁹ - or *block copolymers* possessing distinct blocks displaying each a distinct LCST and UCST behavior (see for example the first examples described in the literature: 50,51,52). Compared to these examples, PCEAm combines several advantages: it is a homopolymer produced from a simple monomer obtained in straightforward and robust conditions. In addition, we have shown that the dual thermoresponsiveness can be maintained and even tuned by introducing CMAM units in the polymer chains. The copolymerization of CEAm with the structurally similar CMAM occurred in a random and controlled fashion by RAFT copolymerization. Compared to the PCEAm homopolymer, the window, in which the P(CEAm-*co*-CMAM) is insoluble, is increased over a broader temperature range. Based on these results, we can hypothesize that (i) amide functions enable polymer-polymer

and polymer-water interactions with hydrogen bonding, (ii) cyano functions promote polymer-polymer interactions, (iii) compared to CMAm the presence of an additional methylene group in CEAm units favors side-chain mobility/flexibility reducing polymer-polymer interactions induced by cyano functions.

Finally, we have also shown that the copolymerization of CEAm with very low percentages of Am (> 2 mol%) had a great impact on the thermoresponsiveness of the resulting P(CEAm-co-Am) random copolymer in water.

Currently, our work is directed towards a better understanding of the dual LCST/UCST behavior of the PCEAm homopolymers. We believe that these new (co)polymers pave the way towards a new class of responsive materials. Their dual sharp and reversible transition temperatures make these polymers extremely interesting candidates to engineer smart materials that respond only within a specific range of temperatures rather than just below or beyond a critical value.

Acknowledgements

The authors thank the Sorbonne Université Doctoral School ED397 for funding.

Keywords: *N*-cyanoalkylacrylamide, RAFT polymerization, closed-loop phase diagram, cloud point, clearing point, copolymers, dual thermoresponsive polymers

References

- ¹ D. Roy, W. L. A. Brooks and B. S. Sumerlin, *Chem. Soc. Rev.*, 2013, **42**, 7214–7243.
- ² A. Bordat, T. Boissenot, J. Nicolas, N. Tsapis, *Adv. Drug Deliv. Rev.*, 2019, **138**, 167–192.
- ³ S. Li, X. J. Wang, S. Zhang, J. B. Hu, Y. L. Du, X. Q. Kang, X. L. Xu, X. Y. Ying, J. You and Y. Z. Du, *Biomaterials*, 2017, **131**, 36–46.
- ⁴ J. Seuring and S. Agarwal, *Macromol. Rapid Commun.*, 2012, **33**, 1898–1920.
- ⁵ J. Seuring and S. Agarwal, *ACS Macro Lett.*, 2013, **2**, 597–600.
- ⁶ D. N. Schulz, D. G. Peiffer, P. K. Agarwal, J. Larabee, J. J. Kaladas, L. Soni, B. Handwerker and R. T. Garner, *Polymer*, 1986, **27**, 1734–1742.
- ⁷ T. Maji, S. Banerjee, Y. Biswas and T. K. Mandal, *Macromolecules*, 2015, **48**, 4957–4966.
- ⁸ J. Seuring and S. Agarwal, *Macromol. Chem. Phys.*, 2010, **211**, 2109–2117.
- ⁹ J. Seuring and S. Agarwal, *Macromolecules*, 2012, **45**, 3910–3918.
- ¹⁰ G. Meiswinkel and H. Ritter, *Macromol. Rapid Commun.*, 2013, **34**, 1026–1031.
- ¹¹ T. Aoki, K. Nakamura, K. Sanui, A. Kikuchi, T. Okano, Y. Sakurai and N. Ogata, *Polym. J.*, 1999, **31**, 1185–1188.
- ¹² N. Shimada, H. Ino, K. Maie, M. Nakayama, A. Kano and A. Maruyama, *Biomacromolecules*, 2011, **12**, 3418–3422.
- ¹³ C. Xing, Z. Shi, J. Tian, J. Sun and Z. Li, *Biomacromolecules*, 2018, **19**, 2109–2116.
- ¹⁴ A. Augé, F. Camerel, A. Benoist and Y. Zhao, *Polym. Chem.*, 2020, **11**, 3863–3875.
- ¹⁵ C. Zhou, Y. Chen, M. Huang, Y. Ling, L. Yang, G. Zhao and J. Chen, *New J. Chem.*, 2020, **44**, 14551–14559.
- ¹⁶ A. Augé and Y. Zhao, *RSC Adv.*, 2016, **6**, 70616–70623.

-
- ¹⁷ L. Wu, L. Zong, H. Ni, X. Liu, W. Wen, L. Feng, J. Cao, X. Qi, Y. Ge and S. Shen, *Biomater. Sci.*, 2019, **7**, 2134–2143.
- ¹⁸ P. Lertturongchai, M. I. A. Ibrahim, A. Durand, P. Sunintaboon and K. Ferji, *Macromol. Rapid Commun.*, 2020, **41**, 2000058.
- ¹⁹ N. Audureau, F. Coumes, J.-M. Guigner, T. P. T. Nguyen, C. Ménager, F. Stoffelbach and J. Rieger, *Polym. Chem.*, 2020, **11**, 5998–6008.
- ²⁰ C. Otsuka, Y. Wakahara, K. Okabe, J. Sakata, M. Okuyama, A. Hayashi, H. Tokuyama and S. Uchiyama, *Macromolecules*, 2019, **52**, 7646–7660.
- ²¹ A. Asadujjaman, B. Kent and A. Bertin, *Soft Matter*, 2017, **13**, 658–669.
- ²² A. Chapiro and L. Perec-Spritzer, *Eur. Polym. J.*, 1975, **11**, 59–69.
- ²³ N. Audureau, C. Veith, F. Coumes, T. P. T. Nguyen, J. Rieger and F. Stoffelbach, *Macromol Rapid Commun.*, 2021, **42**, 2100556.
- ²⁴ N. Audureau, F. Coumes, C. Veith, C. Guibert, J.-M. Guigner, F. Stoffelbach and J. Rieger, *Polymers*, 2021, **13**, 4424.
- ²⁵ D. C. Guth and E. J. Kerle, US 2798059.
- ²⁶ M. Yamatani, K. Haruyama and M. Kijima, JP 2018168209.
- ²⁷ M. Inoue and H. Nagasaki, JP 2011190484.
- ²⁸ H. S. Choi, J. M. Kim, K.-J. Lee and Y. C. Bae, *J. Appl. Polym. Sci.*, 1999, **72**, 1091–1099.
- ²⁹ H. Chirowodza, W. Weber, P. Hartmann and H. Pasch, *Macromol. Symp.*, 2012, **313-314**, 135–145.
- ³⁰ J. Seuring, F. M. Bayer, K. Huber and S. Agarwal, *Macromolecules*, 2012, **45**, 374–384.
- ³¹ F. Liu, J. Seuring and S. Agarwal, *Polym. Chem.*, 2013, **4**, 3123–3131.
- ³² W. Zhang, F. D’Agosto, P.-Y. Dugas, J. Rieger and B. Charleux, *Polymer*, 2013, **54**, 2011–2019.
- ³³ S. Napolitano, E. Glynos and N. B. Tito, *Rep. Prog. Phys.*, 2017, **80**, 036602.

-
- ³⁴ Y. Xia, X. Yin, N. A. D. Burke and H. D. H. Stöver, *Macromolecules*, 2005, **38**, 5937–5943.
- ³⁵ D. G. Lessard, M. Ousalem and X. X. Zhu, *Can. J. Chem.*, 2001, **79**, 1870–1874.
- ³⁶ V. Bütün, S. P. Armes and N. C. Billingham, *Polymer*, 2001, **42**, 5993–6008.
- ³⁷ Q. Li, A. P. Constantinou and T. K. Georgiou, *J. Polym. Sci.*, 2021, **59**, 230–239.
- ³⁸ N. S. Jeong, M. Redhead, C. Bosquillon, C. Alexander, M. Kelland and R. K. O’Reilly, *Macromolecules*, 2011, **44**, 886–893.
- ³⁹ N. S. Jeong, M. Hasan, D. J. Phillips, Y. Saaka, R. K. O’Reilly and M. I. Gibson, *Polym. Chem.*, 2012, **3**, 794–799.
- ⁴⁰ S. Glatzel, A. Laschewsky and J.-F. Lutz, *Macromolecules*, 2011, **44**, 413–415.
- ⁴¹ R. Freitag and F. Garret-Flaudy, *Langmuir*, 2002, **18**, 3434–3440.
- ⁴² J. Lu, X. Zhou, J. Sun, M. Xu, M. Zhang and C. Zhao, *J. Polym. Sci.*, 2021, **59**, 1701–1710.
- ⁴³ J. Chen, Y. Pei, L.-M. Yang, L.-L. Shi and H.-J. Luo, *Macromol. Symp.*, 2005, **225**, 103–111.
- ⁴⁴ R. Longenecker, T. Mu, M. Hanna, N. A. D. Burke and H. D. H. Stöver, *Macromolecules*, 2011, **44**, 8962–8971.
- ⁴⁵ X. Cai, L. Zhong, Y. Su, S. Lin and X. He, *Polym. Chem.*, 2015, **6**, 3875–3884.
- ⁴⁶ M. Li, X. He, Y. Ling and H. Tang, *Polymer*, 2017, **132**, 264–272.
- ⁴⁷ H. Okamura, T. Maruyama, S. Masuda, K. Minagawa, T. Mori and M. Tanaka, *J. Polym. Res.* 2002, **9**, 17–21.
- ⁴⁸ Y. Zhu, R. Batchelor, A. B. Lowe and P. J. Roth, *Macromolecules*, 2016, **49**, 672–680.
- ⁴⁹ T. Shiomi, K. Imai, K., C. Watanabe and M. Miya, *J. Polym. Sci. Polym. Phys. Ed.*, 1984, **22**, 1305–1312.
- ⁵⁰ M. Arotçaréna, B. Heise, S. Ishaya, A. Laschewsky, *J. Am. Chem. Soc.*, 2002, **124**, 3787–3793.
- ⁵¹ J. V. M. Weaver, S. P. Armes and V. Butun, *Chem Commun.*, 2002, **18**, 2122–2123.
- ⁵² Y. Maeda, H. Mochiduki and I. Ikeda, *Macromol. Rapid Commun.* 2004, **25**, 1330–1334.